Inorg. Chem. **2005**, *44*, 7732–7742

Mechanistic Information on the Reductive Elimination from Cationic Trimethylplatinum(IV) Complexes to Form Carbon–Carbon Bonds

Joanna Procelewska,[†] Achim Zahl,[†] GUnter Liehr,[†] Rudi van Eldik,*[,†] Nicole A. Smythe,[‡] B. Scott Williams,[‡,§] and Karen I. Goldberg*[,‡]

Institute for Inorganic Chemistry, University of Erlangen−Nürnberg, Egerlandstrasse 1, 91058 Erlangen, Germany, and Department of Chemistry, University of Washington, Seattle, Washington 98195-1700

Received April 1, 2005

Cationic complexes of the type *fac*-[$(L_2)Pt^{IV}Me_3$(pyr-X)][OTf] (pyr-X = 4-substituted pyridines; L_2 = diphosphine, viz., dppe = bis(diphenylphosphino)ethane and dppbz = *o*-bis(diphenylphosphino)benzene; OTf = trifluoromethanesulfonate) undergo C–C reductive elimination reactions to form [L_2Pt^{II}Me(pyr-X)][OTf] and ethane. Detailed studies indicate that these reactions proceed by a two-step pathway, viz., initial reversible dissociation of the pyridine ligand from the cationic complex to generate a five-coordinate Pt^{IV} intermediate, followed by irreversible concerted C–C bond formation. The reaction is inhibited by pyridine. The highly positive values for $\Delta S^{\ddagger}_{obs}$ = +180 ± 30 J K^{-1} mol^{-1}, $\Delta H^{\ddagger}_{obs}$ = 160 ± 10 kJ mol^{-1}, and $\Delta V^{\ddagger}_{obs}$ = +16 ± 1 cm^3 mol^{-1} can be accounted for in terms of significant bond cleavage and/or partial reduction from Pt^{IV} to Pt^{II} in going from the ground to the transition state. These cationic complexes have provided the first opportunity to carry out detailed studies of C–C reductive elimination from *cationic* Pt^{IV} complexes in a variety of solvents. The absence of a significant solvent effect for this reaction provides strong evidence that the C–C reductive coupling occurs from an unsaturated five-coordinate Pt^{IV} intermediate rather than from a six-coordinate Pt^{IV} solvento species.

Introduction

Platinum(IV) complexes of the type *fac*-[$(L_2)PtMe_3X$], X = halide, carboxylate, aryloxide; L = a monodentate phosphine (PMe_2Ph, $PMePh_2$) or L_2 = a bidentate diphosphine (dppe = bis(diphenylphosphino)ethane, dppbz = *o*-bis(diphenylphosphino)benzene), undergo reductive elimination reactions to form C−C and/or C−heteroatom bonds. These reactions have received significant attention, initially from Puddephatt et al.[1] and more recently from Goldberg and coworkers.[2] These groups performed a series of detailed kinetic studies and found that, for all C−C and C−X reductive elimination reactions from Pt^{IV} investigated, the mechanistic evidence supported a reaction pathway in which dissociation of a ligand occurred prior to the actual reductive coupling. The complexes *fac*-[$(L_2)PtMe_3X$], where L is a monodentate neutral ligand and X a halide or alkyl group, dissociate ligand L, and subsequent C−C reductive coupling is proposed to occur from the resultant five-coordinate intermediate.[1] When L_2 is instead a bidentate phosphine ligand and X is an alkyl group, evidence supports opening of the phosphine chelate to generate an analogous five-coordinate species prior to C−C coupling.[2e,f] For complexes where L_2 is a bidentate neutral bisphosphine ligand and X is I, OAc, or OAr, competitive C−C and C−X reductive elimination is found to proceed via initial dissociation of X^-.[2a−d] Both C−C and C−X coupling reactions of the complexes *fac*-[$(L_2)PtMe_3X$] (L_2 = bidentate phosphine, X = I, OAc, OAr) are proposed to proceed through the same five-coordinate intermediate as shown in Scheme 1.[3]

* To whom correspondence should be addressed. E-mail: vaneldik@chemie.uni-erlangen.de (R.v.E.), goldberg@chem.washington.edu (K.I.G.).
[†] University of Erlangen−Nürnberg.
[‡] University of Washington.
[§] Current address: Joint Science Department, Keck Science Center, Claremont McKenna, Scripps, and Pitzer Colleges, 925 N. Mills Ave., Claremont, CA 91711.

(1) (a) Brown, M. P.; Puddephatt, R. J.; Upton, C. E. E. *J. Chem. Soc., Dalton Trans.* **1974**, 2457. (b) Roy, S.; Puddephatt, R. J.; Scott, J. D. *J. Chem. Soc., Dalton Trans.* **1989**, 2121. (c) Brown, M. P.; Puddephatt, R. J.; Upton, C. E. E. *J. Chem. Soc., Dalton Trans*. **1973**, 49, C61.

(2) Examples for C−C (a−f), C−I (a and b), and C−O (c and d): (a) Goldberg, K. I.; Yan, J.; Winter, E. L. *J. Am. Chem. Soc.* **1994**, *116*, 1573. (b) Goldberg, K. I.; Yan, J.; Breitung, E. M. *J. Am. Chem. Soc.* **1995**, *117*, 6889. (c) Williams, B. S.; Holland, A. W.; Goldberg, K. I. *J. Am. Chem. Soc.* **1999**, *121*, 252. (d) Williams, B. S.; Goldberg, K. I. *J. Am. Chem. Soc.* **2001**, *123*, 2576. (e) Crumpton, D. M.; Goldberg, K. I. *J. Am. Chem. Soc.* **2000**, *122*, 962. (f) Crumpton-Bregel, D. M.; Goldberg, K. I. *J. Am. Chem. Soc.* **2003**, *125*, 9442.

10.1021/ic050478+ CCC: $30.25
Published on Web 10/04/2005

Scheme 1

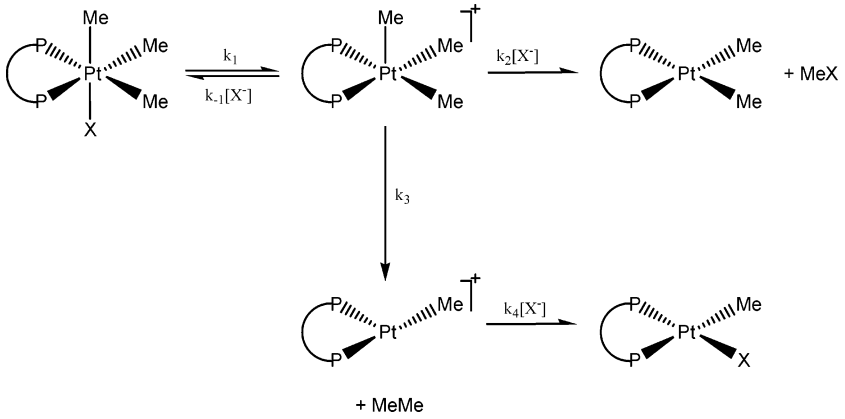

Consistent with this mechanism, rates of reductive elimination from *fac*-[$(L_2)PtMe_3X$] (L_2 = bidentate phosphine, X = I, OAc, OAr) are increased by factors that enhance the dissociation of the anionic X group from the six-coordinate reactant. Thus, the incorporation of electron-withdrawing groups into X, the addition of Lewis acids to the solution, and the use of more polar solvents all increase the overall reaction rate.[2] Notably, these factors tend to enhance C−C coupling more than C−X coupling because they increase the equilibrium constant for X anion dissociation ($k_1/k_{-1} = K_1$) and at the same time decrease the effective rate constant for nucleophilic attack of the dissociated X^- anion on the electrophilic Pt^{IV}-bound methyl carbon in the intermediate complex (k_2). Hence, variation of reaction conditions can be effectively used to select for either C−X or C−C coupled products.

We have recently extended the study of reductive elimination reactions from these types of complexes to the cationic species *fac*-{$[(L_2)Pt^{IV}Me_3(pyr\text{-}X)][OTf]$}, L_2 = dppe and dppbz, with pyridine (pyr) and its 4-substituted analogues NC_5H_4X (pyr-X). In contrast to the *fac*-$[(L_2)Pt^{IV}Me_3(X)]$ complexes previously studied (L_2 = bidentate phosphine and X = I, OAc, OPh), these ionic complexes undergo reductive elimination to form exclusively C−C coupling products, viz., ethane and $[L_2Pt^{II}Me(pyr\text{-}X)][OTf]$, in a variety of solvents. Preequilibrium dissociation of the pyridine ligand from the Pt^{IV} complex is shown to be responsible for the inverse dependence of the observed rate constant on the concentration of added pyridine. Such behavior indicates that the reductive elimination reaction involves either a five-coordinate cationic intermediate or a weakly bound six-coordinate solvento complex. In this contribution, we report kinetic parameters under ambient and elevated pressure in various solvents and discuss their mechanistic implications. The selected complexes provide an important opportunity to investigate C−C reductive elimination from cationic Pt^{IV} centers in a variety of solvents without competing C−heteroatom reductive elimination and so contribute to the further mechanistic understanding of the intimate mechanism of the C−C coupling reaction. Of particular note, the question of whether a six-coordinate solvento species is on the reaction pathway is addressed.

(3) In the case of X = I, Scheme 1 should contain a k_2 term because the reductive elimination of MeI from *fac*-(dppe)$PtMe_3I$ was found to be reversible.

Experimental Section

General Procedures. All transformations were carried out under an Ar atmosphere using standard Schlenk techniques, under an Ar atmosphere in a drybox, or under vacuum. Deuterated THF and benzene were distilled under Ar from sodium/benzophenone ketyl. Acetone was dried over $CaSO_4$ and stored over 4-Å sieves. *o*-Bis-(diphenylphosphino)benzene (dppbz) and bis(diphenylphosphino)-ethane (dppe) were purchased from Aldrich and were used as provided. $[PtMe_3I]_4$, *fac*-[(dppe)$PtMe_3I$], and *fac*-[(dppbz)$PtMe_3I$][4] were prepared by established literature procedures.[5] Celite was dried for 3 days at 180 °C under vacuum.

NMR spectra were acquired on a Bruker Avance DRX 400WB or DPX 300 spectrometer. ^1H and ^{13}C NMR spectra were referenced by using residual protiated solvent peaks, and chemical shifts are reported in ppm relative to tetramethylsilane. ^{31}P NMR spectra were referenced to external H_3PO_4 (0 ppm). For the high-pressure studies, the DRX 400WB spectrometer was used together with a homemade high-pressure probe.[6] The high-pressure NMR tube was sealed with a MACOR plug and an O-ring made of Viton. The plug and O-ring were shown to be stable in the employed solvent. The spectra were evaluated (Fourier transformed and integrated) using the WIN NMR program package. Reactions were monitored by the disappearance of the axial methyl group of the Pt^{IV} starting material relative to ferrocene (T_1 = 50 s, pulses spaced 300 s apart).

In Situ Generation of *fac*-[(dppe)$PtMe_3$(pyr)][OTf] ($1a_0$) for Kinetic Experiments. *fac*-[(dppe)$PtMe_3I$] (311.2 mg, 0.407 mmol) was suspended in chilled acetone-d_6 with ferrocene used as the internal standard (50 mL, −40 °C), and AgOTf (Aldrich, 121 mg, 0.470 mmol) was added slowly to the solution containing an equivalent amount of pyridine and stirred vigorously. Because all kinetic experiments were carried out with an excess of 20% AgOTf, control experiments were performed to show that the presence of AgOTf does not affect the reaction rates.[7] The yellow-silver iodide precipitate immediately became visible and was removed after ca. 5 min by vacuum filtration through a fine-porosity filter (Spartan,

(4) This complex has been characterized crystallographically: see the Supporting Information.
(5) (a) Appleton, T. G.; Bennett, M. A.; Tomkins, B. *J. Chem. Soc., Dalton Trans.* **1976**, 439. (b) Clark, H. C.; Manzer, L. E. *J. Organomet. Chem.* **1973**, *59*, 411.
(6) Zahl, A.; Neubrand, A.; Aygen, S.; van Eldik, R. *Rev. Sci. Instrum.* **1994**, *65*, 882.
(7) See the Supporting Information.

30/0.2 RC). The solution was stored in liquid nitrogen when not being actively monitored. For a typical kinetic run, 1 mL of solution was transferred under an Ar atmosphere to a Wilmad screw-cap NMR tube equipped with a poly(tetrafluoroethylene) septum. A measured amount of pyridine (Aldrich, 99.9%) was added using a microliter syringe. The NMR tube was then heated to the required temperature, and after the kinetic run, the mass balance was confirmed by integration of products against the internal ferrocene standard. At low temperature, the ^{1}H and ^{31}P{^{1}H} NMR spectra of complex **1a$_0$** exhibit the pattern typical for a complex with a *fac*-[(L$_2$)PtMe$_3$(X)] arrangement with two sets of methylplatinum resonances in a 1:2 ratio, at δ 0.13 (t w/satellites, $^2J_{PtH}$ = 66.6 Hz, $^3J_{PH}$ = 7.7 Hz, Pt−CH_3 trans to pyridine) and 1.32 (t w/satellites, $^2J_{PtH}$ = 55.4 Hz, $^3J_{PH}$ = 6.6 Hz, Pt−CH_3 cis to pyridine), respectively.[8]

In Situ Preparation of *fac*-[(dppe)PtMe$_3$(*p*-NC$_5$H$_4$X)][OTf] (1a$_{1-4}$) for Kinetic Experiments. All of the pyridine complexes *fac*-[(dppe)PtMe$_3$(*p*-NC$_5$H$_4$X)][OTf], X = NH$_2$ (**1a$_1$**), Me (**1a$_2$**), Ph (**1a$_3$**), and CN (**1a$_4$**), and *fac*-[(dppbz)PtMe$_3$(NC$_5$H$_5$)][OTf] (**3a**) were prepared in a fashion analogous to that given for the preparation of **1a$_0$** in situ above. NMR data for these complexes are provided in Table S1 in the Supporting Information. After a kinetic run, the product solution was layered with pentane and cooled to −40 °C. After a few days, crystals were collected, washed with pentane, and dried under vacuum. NMR data for the product complexes **2a$_{1-4}$** are provided in Table S2 in the Supporting Information.

Thermolysis of *fac*-(dppe)PtMe$_3$I in Pyridine-d_5. An NMR tube loaded with *fac*-(dppe)PtMe$_3$I (4 mg, 0.005 mmol) was charged with pyridine-d_5 (300 μL) and sealed on the vacuum line. Peaks due to *fac*-[(dppe)PtMe$_3$(NC$_5$D$_5$)]I were immediately apparent and gradually came to equilibrium with those for *fac*-[(dppe)PtMe$_3$I] (a ratio of ca. 2:1). ^{31}P{^{1}H} NMR for *fac*-[dppePtMe$_3$(NC$_5$D$_5$)]I: δ 17.2 (s w/satellites, $^1J_{PtP}$ = 1124 Hz). ^{1}H NMR for [(dppe)PtMe$_3$-(NC$_5$D$_5$)]I: 0.30 (t w/satellites, $^2J_{PtH}$ = 66.8 Hz, $^3J_{PH}$ = 7.9 Hz, Pt−CH_3 trans to pyridine), 1.42 (t w/satellites, $^2J_{PtH}$ = 55.2 Hz, $^3J_{PH}$ = 6.6 Hz, Pt−CH_3 cis to pyridine). A second sample was prepared in the same fashion as described above and heated for 90 min at 79 °C, after which time the NMR spectrum indicated that the reaction had proceeded quantitatively to the dimethyl species (dppe)PtMe$_2$. ^{31}P{^{1}H} NMR: δ 48.3 (s w/Pt satellites, $^1J_{PtP}$ = 1805 Hz). ^{1}H NMR: δ 1.31 (t, w/Pt satellites, $^2J_{PtH}$ = 70.4, $^3J_{PH}$ = 7.1, PtCH_3), 2.4 (m, PCH_2CH_2P), 7.4 and 7.9 (both m, phenyl groups on phosphine), and *N*-methylpyridinium iodide (δ 4.70, identical with the authentic sample generated from iodomethane and pyridine).

Preparation of *fac*-[(dppe)PtMe$_3$(pyr)][OTf] (1a$_0$). An NMR tube was charged with [(dppe)PtMe$_3$I] (50.2 mg, 0.066 mmol), AgOTf (17 mg, 0.066 mmol), and pyridine (0.5 mL). Solids precipitated, and the material was filtered through glass wool. NMR spectroscopy indicated the formation of a new complex (**1a$_0$**). ^{31}P-{^{1}H} NMR (pyr-d_5): 15.8 (s w/satellites, $^1J_{PtP}$ =1125 Hz). ^{1}H NMR: δ 0.28 (t w/Pt satellites, $^2J_{PtH}$ = 66 Hz, $^3J_{PH}$ = 8.0 Hz, Pt−CH_3 trans to pyridine), 1.42 (t w/satellites, $^2J_{PtH}$ = 48 Hz, $^3J_{PH}$ = 6.0 Hz, Pt−CH_3 cis to pyridine). The reaction volume was reduced and the product precipitated with *n*-pentane (40.6 mg, 71% yield). Anal. Calcd for C$_{35}$H$_{38}$F$_3$NO$_3$P$_2$PtS: C, 48.50; H, 4.42; N, 1.62. Found: C, 48.76; H, 4.49; N, 1.57.

X-ray Crystal Structure Determinations. Colorless rhombohedral crystals of **2a**·C$_6$H$_6$ were grown by slow evaporation of a benzene solution, exposed to air, at ambient temperature. Intensity data were collected on a Nonius CAD4 Mach3 diffractometer with graphite monochromated Mo Kα radiation in the $\omega/2\theta$ scan mode at room temperature (Table 1). The structure was solved by direct methods using SIR-97[9] and refined by full-matrix least-squares on F^2 using SHELXL-97.[10] For further information, see Tables S3−S11 in the Supporting Information.

Table 1. Crystal Structural Information for [(dppe)PtMe(pyr)][OTf]·C$_6$H$_6$

empirical formula	C$_{39}$H$_{38}$NP$_2$PtSO$_3$F$_3$
formula weight	914.82
temperature	210 K
wavelength	0.709 30 Å
crystal system	monoclinic
space group	*P*21/*c*
unit cell dimensions	a = 13.0610(10) Å, α = 90°
	b = 15.616(3) Å, β = 100.303(10)°
	c = 19.295(3) Å, γ = 90°
Vol., Z	3872.0(10) Å^3, 4
density (calculated)	1.564 g/cm^3
absorption coefficient	3.8 mm^{-1}
F(000)	1804
crystal size	0.38 × 0.35 × 0.05 mm
θ range for data collection	2.05−25.5°
limiting indices	−15:15; 0:18; −23:23
reflections collected	5437
independent reflections	7206, R_{int}=0.097

Results and Discussion

Synthesis of *fac*-[(L$_2$)PtMe$_3$(pyr-X)][OTf] Complexes. The platinum(IV) pyridine complex **1a$_0$** was prepared by the reaction of *fac*-[(dppe)PtMe$_3$I] with AgOTf and pyridine in acetone-d_6 at low temperature. This complex undergoes a facile reductive elimination reaction to produce ethane and [(dppe)PtMe(pyr)][OTf] (**2a**) as the only products. The

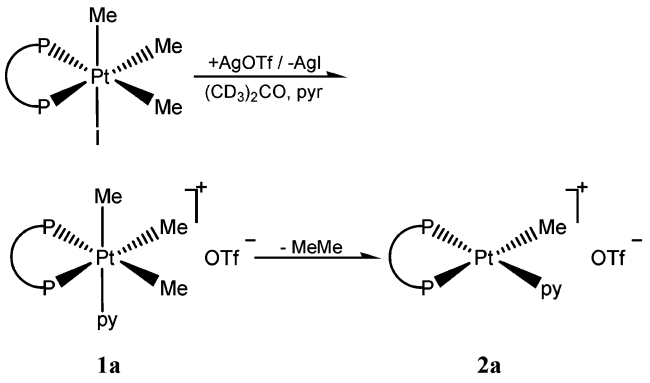

1a **2a**

analogous bis(diphenylphosphino)benzene complex **3a** was prepared in the same manner as **1a$_0$** by the reaction of *fac*-[(dppbz)PtMe$_3$I][12] with AgOTf and pyridine in acetone-d_6.

Characterization of 2a. Filtration and evaporation of the solution after reaction gave **2a**, which was fully characterized

(8) Full ^{1}H NMR data can be found in the Supporting Information.

(9) Altomare, A.; Cascarano, G.; Giacovazzo, C.; Gagliardi, A.; Burla, M. C.; Polidori, G.; Cavalli, M. SIR-92-Program Package for Solvine Crystal Structures by Direct Methods. *J. Appl. Crystallogr.* **1994**, *27*, 435.

(10) Sheldrick, G. M. *SHELXL-97*; University of Göttingen: Göttingen, Germany, 1997. (a) Sheldrick, G. M. *Acta Crystallogr., Sect. A* **1990**, *46*, 467. (b) Sheldrick, G. M. *Acta Crystallogr., Sect. D* **1993**, *49*, 18. (c) Sheldrick, G. M.; Schneider, T. R. *Methods Enzymol.* **1997**, *227*, 319.

(11) The NMR data for **2a** is in the Supporting Information.

(12) See the Supporting Information for a complete listing of bond lengths and angles, atomic coordinates, and displacement parameters.

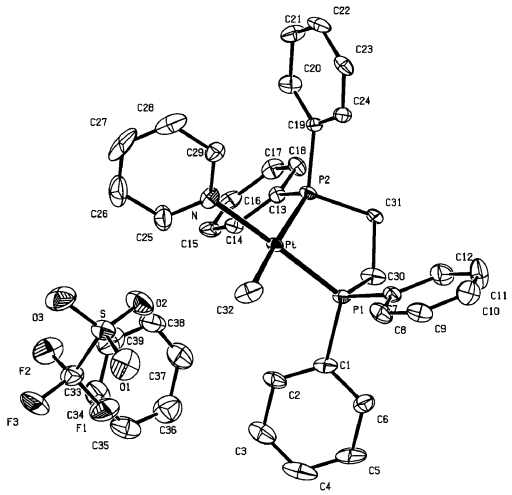

Figure 1. ORTEP diagram of [(dppe)PtMe(pyr)][OTf] showing the labeling of the non-H atoms.

Table 2. Selected Bond Lengths and Angles for the Crystal Structure in Figure 1

bond lengths, Å		bond angles, deg	
Pt−P1	2.239(2)	P1−Pt−P2	86.51(7)
Pt−P2	2.335(2)	P1−Pt−C32	91.2(3)
Pt−N	2.137(7)	N−Pt−C32	85.3(3)
Pt−C32	2.142(8)	P2−Pt−N	96.98(18)
P1−C30	1.865(8)	Pt−P1−C30	108.1(3)
P2−C31	1.874(8)	Pt−P2−C31	106.8(3)
C30−C31	1.566(11)	P1−C30−C31	109.7(5)
		P2−C31−C30	106.8(5)
		C1−P1−C7	105.5(4)
		C13−P2−C19	108.1(4)
		C32−Pt−P2	176.7(3)
		N−Pt−P1	176.52(18)

by NMR spectroscopy, elemental analysis, and X-ray crystallography.[11] A colorless crystal was grown by slow evaporation of a benzene solution of **2a** in air and contains a benzene molecule in the unit cell (Figure S1 in the Supporting Information). The ORTEP diagram of **2a** is shown in Figure 1, and selected bond distances and angles are summarized in Table 2.[12] The geometry at the platinum center is close to square planar. The strong trans influence of the methyl ligand and weak coordination of the pyridine are clearly evident from the differing values of the Pt−P bond lengths (2.335(2) and 2.239(2) Å, respectively) and the $^1J_{PtP}$ coupling constants (1714 and 3732 Hz, respectively; see Figure S1 in the Supporting Information) in $CDCl_3$.

Thermolysis of $1a_0$. Ethane elimination from $\mathbf{1a_0}$ was monitored by ^{1}H NMR spectroscopy, using the decrease and increase in the intensity of signals due to the platinum-bound methyl groups of $\mathbf{1a_0}$ and **2a**, respectively, as shown in Figure 2b. From the speciation diagram (Figure 2a) and the good isosbestic behavior (Figure 3), it is evident that no additional detectable species are formed during the reaction.

Reactions were performed in acetone-d_6, THF-d_8, and benzene-d_6. Each kinetic run showed excellent first-order behavior (observed rate constants as a function of the pyridine concentration, temperature and pressure are reported in the Supporting Information). To obtain kinetic data, NMR spectra were recorded through at least 3 half-lives of the reaction and a reproducible observed rate constant independent of the initial complex concentration was obtained. In control experiments, it was shown that changing the ionic strength of the solution by the addition of varying amounts of LiOTf (Aldrich) to an acetone-d_6 solution of **1a** had a negligible effect on the observed rate constant.[7]

Mechanism of Reductive Elimination Leading to C−C Bond Formation. In preliminary experiments, it was found that the presence of pyridine slowed the rate of the reductive elimination reaction. Therefore, a detailed study of the observed rate constant, k_{obs}, for ethane elimination from $[(dppe)PtMe_3(pyr)]^+$ as a function of the pyridine concentration was undertaken (Figure 4).

The kinetic data were initially fitted with the kinetic expression defined in eq 1, a two-term rate law in which one term is retarded by the free pyridine concentration and the other not. In this equation, k_a represents the rate constant for the direct reductive elimination from the six-coordinate pyridine complex. However, in the presence of a high

$$k_{obs} = k_a + \frac{k_1 k_2}{k_{-1}[pyr] + k_2} \qquad (1)$$

concentration of pyridine, the observed rate constant is greatly decreased, approaching a limiting value of $k_a = (3 \pm 3) \times 10^{-9}$ s^{-1} at 35 °C (determined by extrapolation to infinite [pyr]), which is effectively zero. The essentially

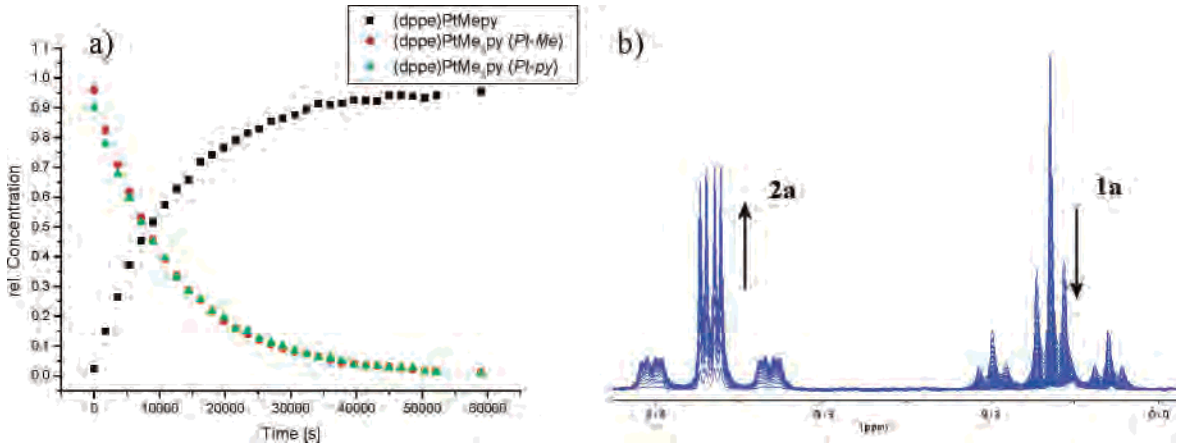

Figure 2. (a) Speciation diagram (concentrations of species versus time). (b) ^{1}H NMR spectrum of platinum-bound methyl groups in acetone-d_6.

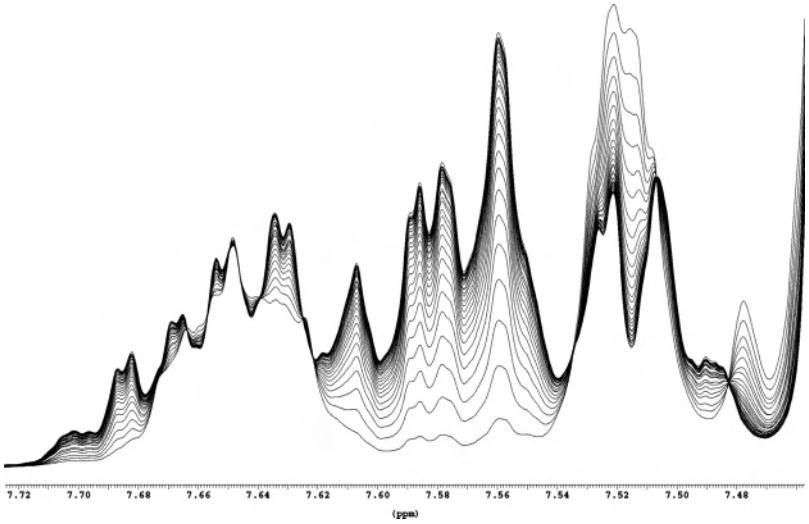

Figure 3. ^{1}H NMR spectrum of a solution of **1a$_0$** in acetone-d_6 as a function of time.

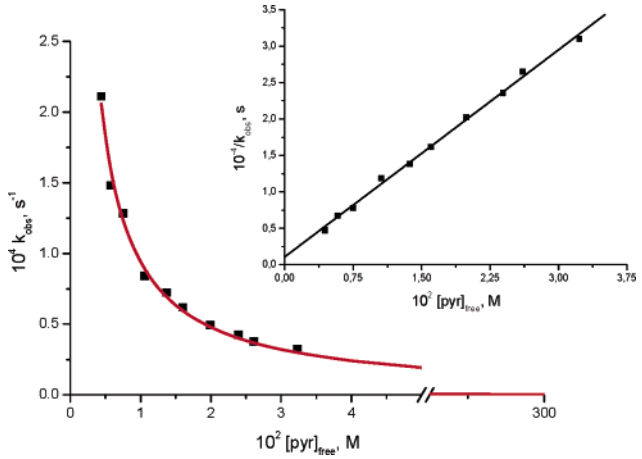

Figure 4. Plot of the observed first-order rate constant versus pyridine concentration for reductive elimination of ethane from *fac*-[(dppe)PtMe$_3$(pyr)][OTf] (**1a$_0$**) in acetone-d_6 at 35 °C. The inset shows the corresponding plot of k_{obs}^{-1} versus [pyridine] according to eq 3.

complete inhibition of the reaction by the addition of an excess of pyridine led us to use eq 2, in which any contribution from a k_a term is neglected. This rate law is consistent with the reaction mechanism shown in Scheme 2. An alternative form of eq 2 is eq 3, which was used to fit the data in Figure 4. By plotting $1/k_{obs}$ vs [pyr] (Figure 4),

$$k_{obs} = \frac{k_1 k_2}{k_{-1}[pyr] + k_2} \quad (2)$$

$$\frac{1}{k_{obs}} = \frac{1}{k_1} + \frac{k_{-1}[pyr]}{k_1 k_2} \quad (3)$$

we were able to obtain the ratio of the rate constant of the binding of pyridine, k_{-1}, to that of C−C coupling, k_2, from the slope of the line ($k_{-1}/k_2 = 880 \pm 20$ M^{-1}, 35 °C) and the rate constant for the dissociation of pyridine ($k_1 = 9 \pm 3 \times 10\text{-}^4$ s^{-1}, 35 °C) from the intercept.

Further simplification of the steady-state expression is possible at high concentrations of pyridine, for which $880[pyr] \gg 1$. Under these conditions, eq 2 reduces to $k_{obs} = k_2 k_1/k_{-1}[pyr] = k_2 K_1/[pyr]$. The formation of ethane is then rate-determining, following the preequilibration between **1a$_0$** and the five-coordinate (or a six-coordinate solvento) intermediate. Because in the absence of added pyridine the reaction at room temperature was too fast to be followed on the NMR time scale, the measurements were performed in

Scheme 2. Proposed Reaction Mechanism for the Reductive Elimination Reaction

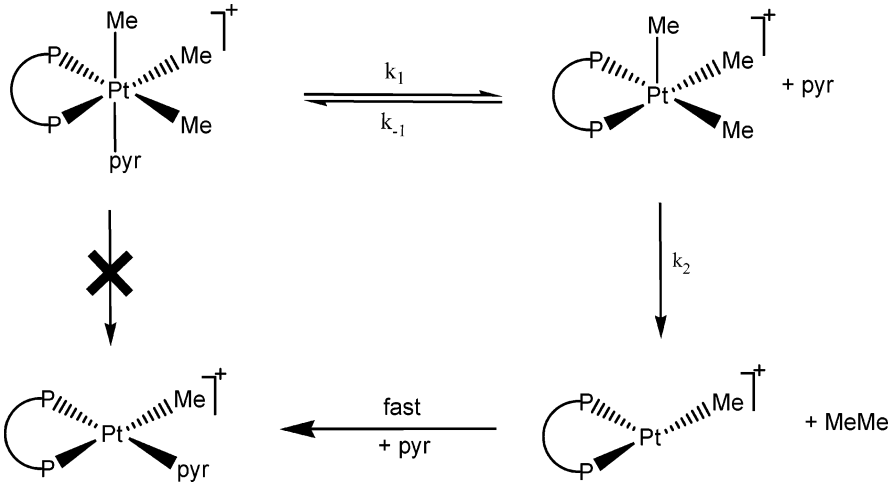

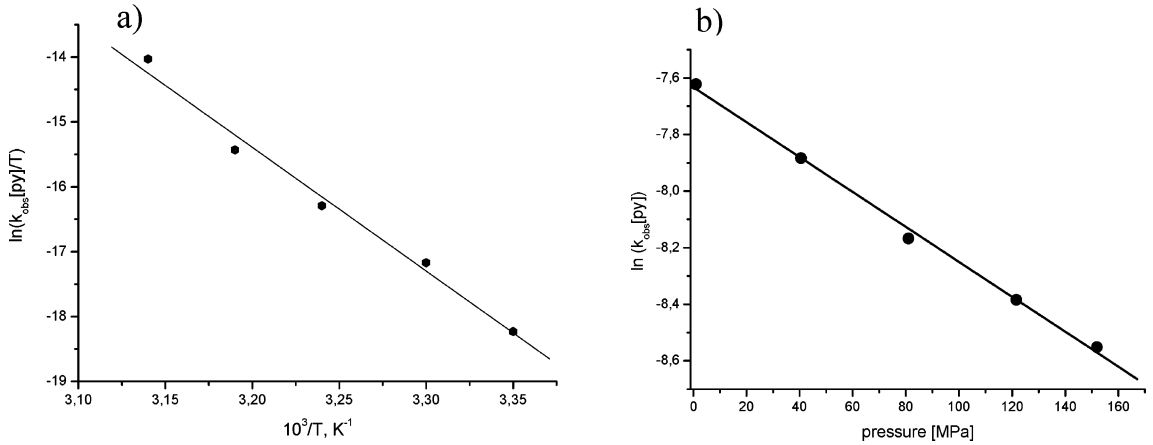

Figure 5. Effect of (a) temperature and (b) pressure at 44 °C on the reductive elimination reaction of $\mathbf{1a_0}$. Experimental conditions: [Pt] = 0.3 mM, [pyr] = 35 mM, solvent = acetone-d_6.

Table 3. Kinetic Comparison of Ethane Reductive Elimination from *fac*-[$(L_2)PtMe_3X$] Complexes Recalculated from the Data Reported in ref 1a

X	L	k_{obs}[a] at 298 K, s^{-1}	solvent	$\Delta G^{\ddagger}$(298 K), kJ mol^{-1}	$\Delta H^{\ddagger}$, kJ mol^{-1}	$\Delta S^{\ddagger}$, J K^{-1} mol^{-1}
Cl	PMe_2Ph	4.4×10^{-7}	dioxane	110 ± 23	112 ± 13	$+6 \pm 35$
Br	PMe_2Ph	2.2×10^{-7}	dioxane	112 ± 4	126 ± 2	$+47 \pm 6$
I	PMe_2Ph	1.4×10^{-7}	dioxane	113 ± 5	140 ± 3	$+90 \pm 8$
I	$PMePh_2$	1.4×10^{-4}	dioxane	96 ± 25	182 ± 13	$+289 \pm 42$
NC_5H_5	$^1/_2$dppe	2.1×10^{-6}	acetone-d_6	106 ± 19	160 ± 10	$+180 \pm 30$

[a] Calculated from the derived activation parameters reported in ref 1a (see the Supporting Information).

the presence of added pyridine (12.5−40.5 mM). Thus, over the entire concentration range investigated, the pyridine concentration is such that 880[pyr] ≫ 1, and the observed rate constant is described by $k_{obs} = k_2K_1/[pyr]$.

Additional evidence that pyridine dissociation is kinetically competent as a preliminary reaction step was provided by monitoring a solution of $\mathbf{1a_0}$ at low temperature by ^{1}H NMR spectroscopy. When NC_5D_5 was added to a solution of $\mathbf{1a_0}$ in acetone-d_6 at −40 °C, a decrease in the intensity of bound pyridine signals was observed without a change in the intensity of the methyl signals, indicating that pyridine exchange is rapid relative to reductive C−C coupling.[13] Hence, the mechanism for C−C reductive elimination should be viewed as a rapid preequilibrium involving the release of pyridine, followed by rate-determining C−C coupling.

Activation Parameters. The thermal activation parameters $\Delta H^{\ddagger}(k_2K_1)$ and $\Delta S^{\ddagger}(k_2K_1)$ were calculated from the temperature dependence (25−45 °C) of k_{obs}[pyr] = k_2K_1 in acetone-d_6. In terms of the empirical rate law under such conditions, it follows that $\Delta H^{\ddagger}(k_2K_1) = \Delta H(K_1) + \Delta H^{\ddagger}(k_2) = 160 \pm 10$ kJ mol^{-1} and $\Delta S^{\ddagger}(k_2K_1) = \Delta S(K_1) + \Delta S^{\ddagger}(k_2) = +180 \pm 30$ J K^{-1} mol^{-1} (Figure 5a; data reported in Table S12 in the Supporting Information).

Our results provide the opportunity to compare the rate and activation parameters for the reductive elimination reaction of ethane from *cationic* and analogous *neutral* Pt^{IV} complexes, the latter published by Puddephatt and coworkers in 1974.[1a] Their mechanistic studies for C−C reductive elimination from the trimethyl halide complexes containing a neutral monodentate ligand, *fac*-[$(L_2)PtMe_3X$] (X = halide; L = a monodentate phosphine), led to a proposal of preliminary phosphine dissociation, followed by concerted C−C coupling from a five-coordinate intermediate as the dominant reaction pathway. The positive activation entropies summarized in Table 3 are in line with the proposed dissociation of a ligand as a preliminary reaction step. As can be seen from the data presented, the activation parameters for C−C reductive elimination from the cationic complex $\mathbf{1a_0}$ are within the range of those reported previously for ethane elimination from the neutral *fac*-[$(L_2)PtMe_3X$] species, supporting the thesis of a similar mechanism involving preliminary dissociation of a neutral ancillary ligand prior to C−C coupling.

In an effort to gain more insight into the intimate reaction mechanism, a systematic pressure dependence study was performed to determine the observed volume of activation, $\Delta V^{\ddagger}(k_2K_1) = -RT[\delta(\ln k_{obs})/\delta p]_T = \Delta V(K_1) + \Delta V^{\ddagger}(k_2)$. The dependence of ln($k_{obs}$) on the applied pressure measured at constant [pyr] was found to be linear in the accessible pressure range, as shown in Figure 5b (data reported in Table S13 in the Supporting Information), which results in $\Delta V^{\ddagger}_{obs} = +16 \pm 1$ cm^3 mol^{-1}. The significantly positive activation volume, a composite value for the contributions from K_1 and k_2 in Scheme 2, is in line with the high positive entropy of activation.

The dissociation of pyridine (K_1 step) should be accompanied by positive entropy and volume changes. From high-pressure studies on pyridine dissociation from octahedral complexes, it is known that an activation volume close to 20 cm^3 mol^{-1} and a correspondingly high positive value for the entropy of activation can be expected.[14] Significant

(13) Intramolecular rapid ligand scrambling about the metal center within [(LL)MMe_3X] complexes is common when either the ligand X or L is readily dissociated, e.g., variable-temperature NMR experiments performed with the complex *fac*-[(bu_2bpy)$PtMe_3$(OTf)]. Hill, G. S.; Yap, G. P. A.; Puddephatt, R. J. *Organometallics* **1999**, *18*, 1408.

(14) Drljaca, A.; Hubbard, C. D.; van Eldik, R. *Chem. Rev.* **1998**, *98*, 2167.

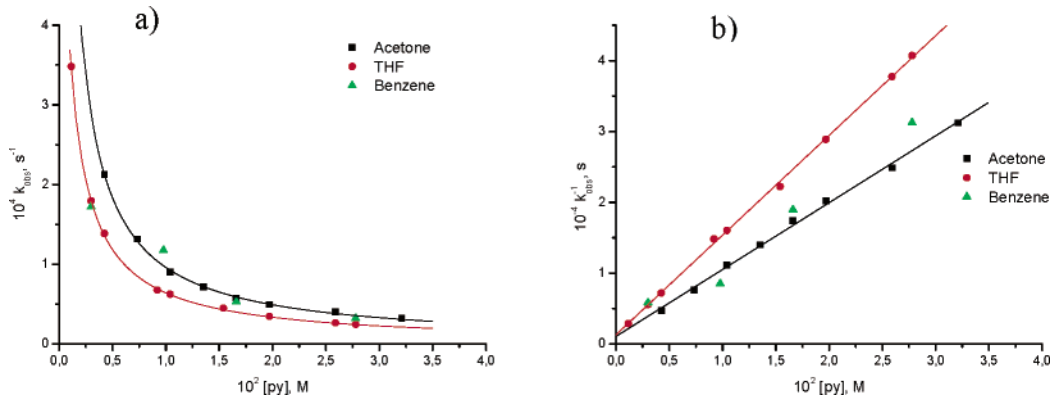

Figure 6. Effect of solvent on the observed rate constant for the reductive elimination of ethane from $\mathbf{1a_0}$ as a function of the pyridine concentration at 35 °C. Data fits are included for acetone and THF as solvents but not for benzene because of the limited number of data points.

positive values are also expected for the reductive elimination step to give ethane (k_2) because the process involves the conversion of the Pt^{IV} complex to the Pt^{II} complex and one molecule of ethane.[16] High positive activation volumes are therefore expected here, especially when the relatively high partial molar volume of ethane of 52.4 cm^3 mol^{-1} is taken into account. High positive activation volumes have been found for other reductive elimination reactions.[15]

Kinetics in Different Solvents. The reductive elimination reaction of ethane from $\mathbf{1a_0}$ was monitored in acetone-d_6, THF-d_8, and benzene-d_6 in order to probe the impact of the solvent polarity and donating ability on the rate of the reaction.[17] In all three solvents, the reaction rate was shown to be inversely proportional to the concentration of pyridine (experimental data reported in Table S15 in the Supporting Information; kinetic plots given in Figure 6).

The lack of a strong dependence of the rate of the reaction on the solvent polarity (see Figure 6b) implies that neither the intermediates nor the transition state is significantly more or less polar that the pyridine starting complex $\mathbf{1a_0}$. By way of comparison, the rate constant for C−C coupling from *fac*-[(dppe)$PtMe_3$OAc], where ionic intermediates are generated along the reaction coordinate, increases approximately 60 times on going from THF to acetone as the solvent.[2d] The relative independence of the reductive elimination from $\mathbf{1a_0}$ on the donating ability of the solvent (the reaction proceeds at roughly the same rate in all three solvents) argues strongly against reductive elimination occurring from a six-coordinate solvento complex and supports the assertion that C−C coupling takes place from the unsaturated five-coordinate Pt^{IV} intermediate.

Exclusive C−C Reductive Elimination from Cationic Pt^{IV} Complexes. It should be noted that the exclusive C−C reductive elimination reaction observed for the cationic complexes of this study differs significantly from the outcome observed upon thermolysis of analogous neutral complexes with chelating phosphine ligands, *fac*-[(L_2)-$PtMe_3X$] (X = OAc, OAr). In the case of these acetate and aryloxide compounds, C−heteroatom coupling generating methyl acetate and methyl aryl ethers was observed in competition with the C−C coupling to produce ethane.[2c,d] The relative amounts of the different reductive elimination products were found to be highly sensitive to the polarity of the solvent, and the C−O-coupled products dominated when the thermolyses were carried out in nonpolar solvents. In contrast, exclusive C−C coupling was observed for the cationic complexes $\mathbf{1a_0}$ with the formation of only ethane and **2a** in both polar and nonpolar solvents.

The absence of C−heteroatom reductive elimination products in the decomposition reaction of $\mathbf{1a_0}$ implies that neither triflate anion nor pyridine is nucleophilic enough to compete with the unimolecular reaction of ethane reductive elimination from the $dppePtMe_3^+$ cation. However, it is interesting that products that would be expected from C−N reductive elimination were observed when the more nucleophilic iodide ion was present in the reaction mixture. Dissolution of *fac*-[(dppe)$PtMe_3$I] at room temperature in pyridine-d_5 resulted in an equilibrium with *fac*-[dppe$PtMe_3$-(pyr-d_5)]I. In contrast to the thermolysis of $\mathbf{1a_0}$, the thermolysis of this solution at 79 °C formed [(dppe)$PtMe_2$] and [Me(pyr-d_5)]I. Presumably, nucleophilic attack of iodide at the Pt^{IV}Me cation occurs as previously described for MeI reductive elimination from *fac*-[(dppe)$PtMe_3$I].[2a,b] Subsequent reaction of MeI with pyridine would then rapidly form methylpyridinium iodide.[18] The latter reaction has been independently verified. Notably, thermolysis of isolated

(15) For example, elimination of H_2 from a ruthenium cluster is characterized by +20 cm^3 mol^{-1}: Venter, J. A.; Leipoldt, J. G.; van Eldik, R. *Inorg. Chem.* **1991**, *30*, 2207.

(16) To ascertain the relative contributions of each mechanistic step to the observed activation parameters for the reaction, we attempted to determine the activation parameters for the k_1 step. The temperature dependence of k_{obs} was studied as a function of [pyridine]. The values of k_{obs} were extrapolated to zero pyridine concentration by linear regression analysis of the plots in Figure S5a in the Supporting Information. These values of k_1 (=k_{obs} at [pyr] = 0 M) were then plotted as a function of temperature. In this way, the activation parameters for k_1 could be estimated, viz., $\Delta H^{\ddagger}(k_1) = 90 \pm 20$ kJ mol^{-1} and $\Delta S^{\ddagger}(k_1) = -20 \pm 60$ J K^{-1} mol^{-1} (Figure S5b in the Supporting Information). Although the observed activation enthalpy is in the appropriate range for pyridine dissociation, the large uncertainty in the $\Delta S^{\ddagger}(k_1)$ value renders it less useful as a mechanistic indicator. The values of the activation parameters for K_1k_2 calculated according to eq 3 from the slope of the concentration dependence at different temperatures (Figure S5a in the Supporting Information) were found to be within the error range of those calculated for the selected pyridine concentration in Figure 5a (see Figure S2 and Table S14 in the Supporting Information).

(17) The larger scatter in the benzene data, k_{obs}(benzene-d_6), can be attributed to the low solubility of the starting complex.

(18) Thompson, H. W.; Clandon, E. E. *J. Chem. Soc.* **1933**, 1237.

Table 4. Hammett Parameters (σ)[19] and Observed Rate Constants at 35 °C for Different Pyridine Derivates ([4-NC_5H_4X] = 78 mM) in Acetone-d_6

complex	*p*-NC_5H_4X	*s*	k_{obs}, s^{-1}
1a$_1$	NH_2	−0.66	$(1.9 \pm 0.3) \times 10^{-6}$
1a$_2$	Me	−0.17	$(1.0 \pm 0.1) \times 10^{-5}$
1a$_3$	Ph	−0.01	$(1.7 \pm 0.1) \times 10^{-5}$
1a$_0$	H	0.00	$(1.8 \pm 0.7) \times 10^{-5}$
1a$_4$	CN	0.89	$(1.5 \pm 0.2) \times 10^{-3}$

[(dppe)$PtMe_3$(pyr)]OTf in neat pyridine-d_5 at 79 °C resulted in exclusive C−C reductive elimination to form ethane and **2a**.

Electronic Effects on the Rate of Reductive Elimination. To determine the dependence of the rate of reductive elimination of ethane on the electronic properties of the platinum-bound nitrogen donor, a series of complexes with uncharged 4-substituted pyridine derivates were prepared: *fac*-[(dppe)$PtMe_3$(4-NC_5H_4X)][OTf]; X = NH_2 (**1a$_1$**), Me (**1a$_2$**), Ph (**1a$_3$**), and CN (**1a$_4$**). These complexes were synthesized in the same manner as **1a$_0$** by the reaction of *fac*-[(dppe)$PtMe_3$I] with AgOTf and the corresponding pyridine derivate in acetone-d_6 and characterized by ^{1}H and ^{31}P NMR spectroscopy at low temperature. The measurements were performed at a high 4-NC_5H_4X concentration (78 mM), where presumably $k_{obs} = K_1k_2/$[4-NC_5H_4X].

The rate constants for C−C reductive elimination from **1a$_{0-4}$** are listed in Table 4. The difference in reactivity between the first and last member of the series spans 3 orders of magnitude. The reaction is considerably faster for more electron-withdrawing substituents, viz., a better leaving group ($k_{obs} = (1.5 \pm 0.2) \times 10^{-3}$ s^{-1} for *p*-CN), than for electron-donating substituents ($k_{obs} = (1.0 \pm 0.1) \times 10^{-5}$ s^{-1} for *p*-Me), presumably because better leaving groups favor the formation of the five-coordinate intermediate. The fluorinated analogue of **1a$_0$**, *fac*-[(dppe)$PtMe_3$(NC_5F_5)][OTf] (**1a$_5$**), was also prepared and found to undergo reductive elimination considerably faster than **1a$_{0-4}$** to form ethane and [(dppe)-$PtMe(NC_5F_5)]^+$ as the only products. The reaction rate was too fast to measure.

The Hammett plot[19] for this reaction (Figure 7) shows a good fit with a positive ρ value of 1.90 with respect to σ values. A similar linear correlation between log(k_{obs}) and σ^- values was observed for C−O reductive elimination from the analogous neutral aryloxide complexes *fac*-[(dppbz)-$PtMe_3$(p-OC_6H_4X)],[2d] in which a related two-step mechanism was proposed. In this case, preliminary dissociation of the OR^- group is followed by rate-determining S_N2 attack on a methyl group of the five-coordinate intermediate. Analysis of the rate law indicates that $\rho = \rho(K_1) + \rho(k_2)$.[20] Hence, any attempt to discuss the effect of changing the aryloxide substituent must take into account that such a change affects both steps and affects each step in an opposite fashion. That is, the effect on the value of k_2 is in the opposite direction as the effect on the value of K_1. Thus, the reported value of

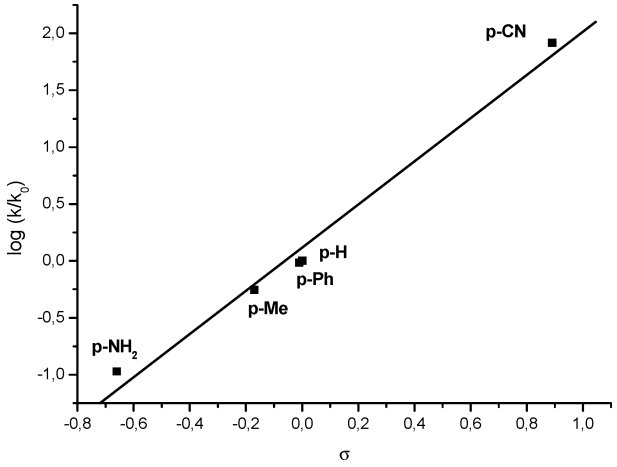

Figure 7. Hammett plot for electronic effects on reductive elimination from **1a$_{0-4}$**.

$\rho = 1.44$ consists of a positive value for $\rho(K_1)$ (crudely estimated from analogous dissociation of phenols in water to be 2.113)[21] and a negative value for $\rho(k_2)$ due to the fact that this is a nucleophilic attack, which should proceed slower with weaker bases (estimated ρ values are in the range −0.771 to −0.994).[21] In the current study, the k_2 step of C−C coupling does not involve pyridine, and thus the ρ value of 1.9 arises purely from K_1. This value of 1.9 is similar to that estimated for the K_1 step in the C−O coupling reaction (2.1) based on the crude organic analogue reaction of phenol ionization in water. In contrast, a significantly higher ρ value of 5.77 has been measured for the ionization of substituted pyridinium ions in water at 25 °C.[22] While variations in the solvent medium and temperature strongly influence ρ values, the inherent differences between a five-coordinate Pt^{IV} center and a proton must also be considered in comparing the organometallic and organic data. For example, contributions from π-back-bonding to the pyridine in complex **1** would be expected to attenuate the organic analogue ρ value.[23]

Kinetic Isotope Effect. The deuterated pyridine-d_5 complex was synthesized in the same manner as **1a$_0$** by the reaction of *fac*-[(dppe)$PtMe_3$I] with AgOTf and deuterated pyridine in acetone-d_6. A value of k_H/k_D of 1.1 ± 0.1 was obtained for the reductive elimination of ethane (at [pyr] = 13.9 mM, $k_{obs\,H} = (7.0 \pm 0.2) \times 10^{-5}$ s^{-1} and $k_{obs\,D} = (6.4 \pm 0.4) \times 10^{-5}$ s^{-1}). A k_H/k_D of 1 is expected for a secondary isotope effect for a reaction in which no orbital hybridization affecting the C−H(D) bond occurs. Such is the case for the proposed mechanism of pyridine dissociation followed by C−C coupling from the five-coordinate intermediate.

Cationic Intermediates. It has been proposed in earlier studies[13] by application of low-temperature ^{1}H, ^{31}P{^{1}H}, and ^{19}F NMR spectroscopy that the cationic complex *fac*-[(dppe)-$PtMe_3]^+$(**1b**) may be present in rapid equilibrium with the

(19) *Advances in Linear Free-Energy Relationships*; Chapman, N. B., Shorer, J., Eds.; Plenum Press: London, 1972.
(20) Exner, O. *Correlation Analysis of Chemical Data*; Plenum Press: New York, 1988; p 70.
(21) *Correlation Analysis in Chemistry: Recent Advances*; Chapman, N. B., Shorter, J., Eds.; Plenum Press: New York, 1978.
(22) The literature values for dissociation of unsubstituted pyridine in water are at 25 °C $\rho(K_{BH+}) = 5.77$ and at 20 °C $\rho(K_{BH+}) = 5.7$. $\rho(K_{BH+}) = 8.47$ at 25 °C in a mixture of 50% ethanol and water is quite different; see ref 21, p 213.
(23) Lavallee, D. K.; Baughman, M. D.; Phillips, M. P. *J. Am. Chem. Soc.* **1977**, *99*, 718.

Scheme 3

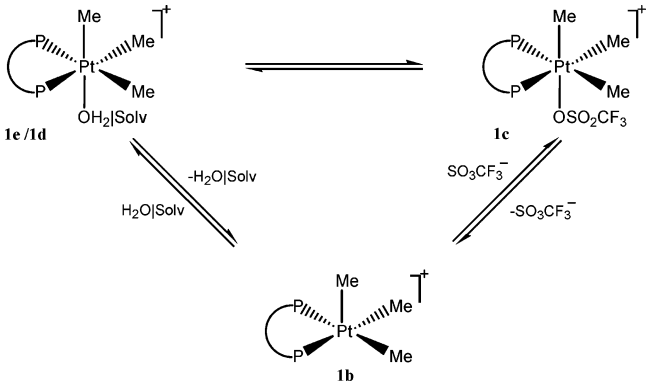

corresponding triflato complex *fac*-[(dppe)PtMe$_3$(OTf)] (**1c**). In addition, dissociation of weakly coordinated OTf^- was shown to be a facile process[24] with evidence presented for a solvento complex, *fac*-[(dppe)PtMe$_3$(solvent)][OTf] (**1d**), in a strong donor solvent, e.g., acetonitrile, and for an aquo complex, *fac*-[(dppe)PtMe$_3$(OH$_2$)][OTf] (**1e**) in a wet solvent (Scheme 3).

A six-coordinate solvento intermediate has also been detected by low-temperature NMR in the oxidative addition of MeI to [(bpy)PtMe$_2$] (bpy = bipyridine) in CD_3CN and to [(bpy)PdMe$_2$] in CD_3CN and acetone-d_6.[25]

Some years ago,[26] van Eldik and co-workers studied the reductive elimination of ethane from the neutral trimethyl iodide complex, [(bpy)Pd^{IV}Me$_3$I], for which preliminary experiments were performed by Canty and co-workers.[25] A detailed study on the effect of the iodide concentration on the reductive elimination process was performed, and a significant deceleration of the reaction rate in the presence of NaI was observed. The mechanism presented in Scheme 4 was suggested.

On the assumption that the displacement of iodide occurs in a rapid preequilibrium (K_1), the rate law for the reactions in Scheme 4 is given by $k_{obs} = (k_a[I^-] + k_bK_1)/([I^-] + K_1)$. The rate and activation parameters for this reaction were measured both in the presence and in the absence of added NaI. It was determined that $k_b \approx 40k_a$ (i.e., ca. 98% of the reductive elimination occurs via path B in the absence of added NaI), $\Delta S^{\ddagger}_A = -66 \pm 34$ J mol^{-1} K^{-1} and $\Delta S^{\ddagger}_B = -53 \pm 25$ J mol^{-1} K^{-1}, and $\Delta V^{\ddagger}_{A,B} = +17 \pm 1$ cm^3 mol^{-1}.[26] The similarity in the activation entropies and volumes of activation measured in the presence and in the absence of NaI led the authors to suggest that ethane elimination occurs from a six-coordinate species in both cases. Thus, C−C coupling was not proposed to occur from the unsaturated five-coordinate intermediate in the absence of added iodide but to a large extent from a very labile six-coordinate solvent complex cation, [(bpy)PdMe$_3$(solvent)]$^+$. Thus, the rapid preequilibrium involves a solvolysis reaction in which iodide is replaced by a weakly coordinating solvent molecule. On the basis of the results presented here, this earlier interpretation should perhaps be revised. A better explanation may be that k_a for this reaction is essentially zero. Note that k_a is very small relative to k_b and the inherent uncertainty in k_a is certainly large enough to accommodate this interpretation. Thus, whether in the presence or in the absence of added iodide, it is distinctly possible that the C−C reductive elimination reaction from (bpy)PdMe$_3$I proceeds exclusively via path B, and as such, there is no compelling argument in favor of the suggested six-coordinate solvento intermediate.

Moreover, the absence of a solvent dependence in our current studies of C−C reductive elimination from **1a$_0$** provides strong evidence in favor of reductive coupling occurring from a five-coordinate cationic intermediate and not a six-coordinate solvated complex. In C−C reductive elimination involving neutral metal complexes that undergo preliminary dissociation of an anionic ligand, a strong solvent dependence on the reaction is expected, based on the involvement of charge separation. Such a dependence of the reaction rate on the solvent has been documented for C−C reductive elimination from the *fac*-[(bpy)PdMe$_3$I] system described above[26] and from *fac*-[(dppe)PtMe$_3$(OR)].[2c,d] However, conclusive studies separating the effects of the differences in polarity and donor ability of the solvents in these reactions were not reported, leaving open the question of the involvement of six-coordinate solvento intermediates. Because pyridine dissociation from the *fac*-[(dppe)PtMe$_3$(pyr)]$^+$ center does not involve charge separation, a strong solvent effect would only be expected if solvent coordination to the platinum center was involved. The similarity in the rates of reductive elimination in benzene-d_6, THF-d_8, and acetone-d_6 argues strongly against the coordination of the solvent on the reaction pathway. The similar kinetic behavior (including a value for k_a (eq 1) that is statistically indistinguishable from zero) and activation volumes between this Pt^{IV} system and that of [(bpy)PdMe$_3$I] ($\Delta V^{\ddagger} = +16$ and $+17$ cm^3 mol^{-1}, respectively) are likely indicative of a common mechanism. Thus, the present study of C−C reductive elimination from cationic Pt^{IV} complexes has provided an enhancement of our previous understanding of C−C coupling from neutral d^6 compounds in which the role of solvent had been heretofore ambiguous.

Spectator Ligand Effect. To study possible effects of the bidentate spectator ligand, similar studies were performed on the analogous complex [(dppbz)PtMe$_3$(pyr)]$^+$ **3a**. As a result of the benzene backbone, dppbz is a more rigid disphosphine chelate than dppe and is expected to have a lesser tendency for dechelation or ring opening.[27] Such ring opening has been implicated in a related example of C−C reductive elimination from Pt^{IV}, in which it was found that C−C reductive elimination was ca. 100 times faster from [(dppe)PtMe$_4$] than from [(dppbz)PtMe$_4$].[2e,f] The dppbz complex **3a** demonstrates strikingly similar behavior to that of the dppe analogue **1a$_0$**. The reaction slows down upon

(24) Hill, G. S.; Rendina, L. M.; Puddephatt, R. J. *J. Chem. Soc., Dalton Trans.* **1996**, 1809.
(25) Byers, P. K.; Canty, A. J.; Crespo, M.; Puddephatt, R. J.; Scott, J. D. *Organometallics* **1988**, *7*, 1363.
(26) Dücker-Benfer, C.; van Eldik, R.; Canty, A. J. *Organometallics* **1994**, *13*, 2412.
(27) (a) Mann, G.; Baranano, D.; Hartwig, J. F.; Rheingold, A. L.; Guzei, I. A. *J. Am. Chem. Soc.* **1998**, *120*, 9205. (b) Sweigart, D. *Inorg. Chim. Acta* **1974**, 317. (c) Dierkes, P.; van Leeuwen, P. W. N. M. *J. Chem. Soc., Dalton Trans.* **1999**, 1519.

Scheme 4

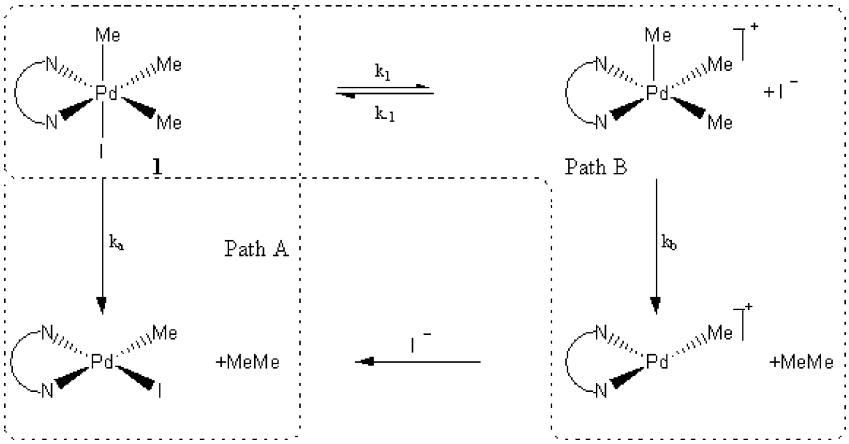

the addition of pyridine, and again the kinetic expression shown as eq 2 is valid (Figure 8).

When the rates of reductive elimination of **1a$_0$** and **3a** are directly compared at the same pyridine concentration (32 mM, 35 °C), it is seen that **1a$_0$** reacts approximately 3.5 times faster than **3a**. This indicates that the spectator ligand in the equatorial plane has a moderate effect on the rate of reductive elimination. In the case of the dppbz complex, the electron-withdrawing capabilities of the benzene backbone could result in a lower electron density on the metal center in comparison to that of the dppe complex. This difference may affect either one or both of the steps in the reductive elimination sequence. In the dppe complex, where the chelate is more saturated, the higher donating character could lead to a larger K_1 value. In addition, the more electron-donating ligand may cause an increase in the reductive coupling step of the reaction, k_2. It should be noted that, in contrast to the difference in rates observed here, the rates of C−O reductive elimination from [(dppe)PtMe$_3$OAc] and [(dppbz)PtMe$_3$OAc] were found to be almost identical.[2d] However, in the case of C−O coupling, the effect of a more electron-donating spectator ligand on the OR^- dissociation (K_1) and on the nucleophilic attack at the Pt−Me group (k_2) should be opposite and so these factors may effectively cancel one another.

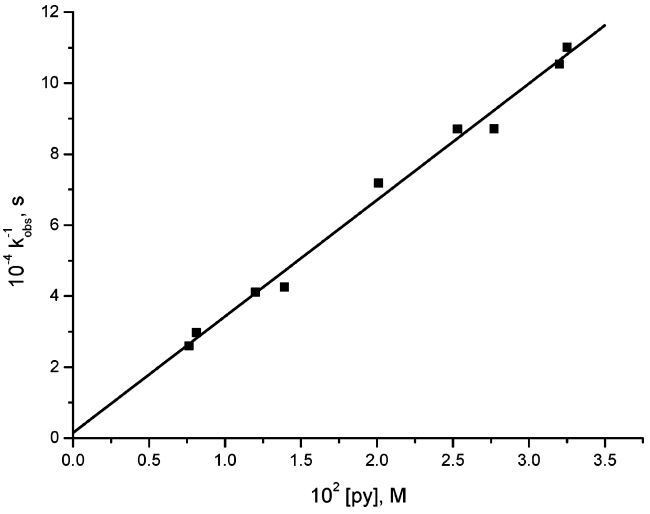

Figure 8. Dependence of the inverse of the observed rate constant on the pyridine concentration for the reductive elimination of ethane from **3a** at 35 °C. $k_1 = (7 \pm 4) \times 10^{-4}$ s^{-1} and $k_{-1}/k_2 = 2160 \pm 80$ M^{-1}.

Conclusions

Detailed mechanistic studies have been performed in order to characterize the reductive elimination reaction to form ethane from a variety of Pt^{IV} complexes of the type *fac*-[(L$_2$)Pt^{IV}Me$_3$(pyr-X)][OTf]. Our mechanistic conclusions fully support the suggested two-step reaction path in Scheme 1 with initial, reversible dissociation of the uncharged pyr-X molecule, followed by rate-determining, concerted elimination of ethane from a five-coordinate intermediate.

The general reaction pattern of formation of an unsaturated intermediate prior to C−C coupling is analogous to that found in previous studies of reductive C−C coupling from related complexes.[1,2] The present work, however, adds a new feature: strong support is presented in favor of the coupling occurring from a true five-coordinate intermediate rather than a possible six-coordinate solvento complex. The lack of an appreciable solvent dependence on the rate of the reaction as the solvent is changed from benzene to acetone, solvents of very different donor abilities, provides compelling evidence for this conclusion. In earlier studies, a pronounced solvent effect on the reaction rate was reported for C−C reductive elimination from the related neutral compounds *fac*-[L$_2$PtMe$_3$X], where L$_2$ is a bidentate phosphine ligand and X is iodide, acetate, or aryloxide,[2a−d] and from *fac*-(bpy)-PdMe$_3$I.[25] For these neutral complexes, reductive coupling to form ethane was preceded by dissociation of an anionic X^- group from the metal center. These reactions proceeded faster in more polar solvents, consistent with a mechanism in which charged intermediates are formed.

In contrast, there is no charge separation when a neutral pyridine ligand dissociates from *fac*-[(L$_2$)Pt^{IV}Me$_3$(pyr-X)]-[OTf] prior to C−C coupling, and so the absence of a solvent effect on the rate of ethane reductive elimination in this system clearly indicates that solvent coordination to the cationic five-coordinate intermediate is not on the reaction coordinate. While a detailed solvent study was not reported for ethane reductive elimination from the neutral complexes

fac-[L_2PtMe_3X], where L = monodentate phosphine and X = halide, which undergo preliminary dissociation of L prior to C−C coupling,[2] the lack of involvement of six-coordinate solvento species in the *cationic* system reported here makes the involvement of such saturated intermediates in the previously reported *neutral* systems highly unlikely. It should also be noted that the activation parameters for the neutral complexes that undergo preliminary dissociation of L are in agreement with those obtained in this study.[1]

The kinetic data obtained in this study suggest a common mechanism for C−C reductive elimination from octahedral Pt^{IV} complexes and confirm the general conclusion that reductive elimination directly from six-coordinate d^6 complexes seems to be kinetically unfavorable and rather the reaction requires ancillary ligand loss to form a five-coordinate complex prior to the rate-determining C−C bond formation step. Five-coordinate platinum(IV) alkyl species have been consistently proposed as key intermediates in numerous studies of the mechanism of reductive elimination/oxidative addition reactions to form or break C−C, C−H, C−O, and C−I bonds at Pt^{IV}/Pt^{II} centers.[2,28] Recently, the first example of an isolable, crystallographically characterized five-coordinate platinum(IV) alkyl complex related to the $[(L_2)PtMe_3]^+$ intermediate was reported.[29,30] The intermediacy of such unsaturated Pt^{IV} species in bond-breaking and bond-making reactions of model Pt complexes has significant implications for their involvement in platinum-catalyzed selective alkane functionalization reactions.[31] Thus, our improved mechanistic understanding of C−C coupling from Pt^{IV}, with compelling evidence for the intermediacy of an *unsaturated* five-coordinate species rather than a six-coordinate intermediate with a coordinated solvent molecule, should be of significant use in current efforts to exploit platinum catalysts for alkane oxidation reactions.

Acknowledgment. The authors gratefully acknowledge financial support from the Deutsche Forschungsgemeinschaft, Fonds der Chemischen Industrie, and National Science Foundation. We thank Prof. U. Fekl (University of Toronto) for supervision of J.P. during preliminary work on this project and for stimulating discussions and also A. Pawlikowski for some experimental assistance on this project. Dr. F. W. Heinemann is thanked for performing the X-ray structure determination of the complex [(dppbz)$PtMe_3$I].

Supporting Information Available: Tables of atom coordinates, thermal parameters, hydrogen atom parameters, bond distances, and bond angles for the complexes [(dppe)PtMe(pyr)][OTf]·C_6H_6 and [(dpppbz)$PtMe_3$I]·0.5$CHCl_3$ and figures of kinetic data and Eyring plots. This material is available free of charge via the Internet at http://pubs.acs.org.

IC050478+

(28) (a) Albrecht, M.; Gossage, R. A.; Spek, A. L.; van Koten, G. *J. Am. Chem. Soc.* **1999**, *121*, 11898. (b) van der Boom, M. E.; Kraatz, H.-B.; Hassner, L.; Ben-David, Y.; Milstein, D. *Organometallics* **1999**, *18*, 3873.

(29) (a) Fekl, U.; Goldberg, K. I. *J. Am. Chem. Soc*. **2002**, *124*, 6804. (b) Fekl, U.; Kaminsky, W.; Goldberg, K. I. *J. Am. Chem. Soc.* **2001**, *123*, 6423.

(30) A related five-coordinate silyl(dihydrido)platinum(IV) complex has also been structurally characterized: Reinartz, S.; White, P.; Brookhart, M.; Templeton, J. L. *J. Am. Chem. Soc.* **2001**, *123*, 6425.

(31) Recent reviews: (a) Labinger, J. A.; Bercaw, J. E. *Nature* **2002**, *417*, 507. (b) Fekl, U.; Goldberg, K. I. *Adv. Inorg. Chem*. **2003**, *54*, 259. (c) Sen, A. *Top. Organomet. Chem*. **1999**, *3*, 80. (d) Crabtree, R. H. *J. Chem. Soc., Dalton Trans*. **2001**, 2437. (e) Shilov, A. E.; Shul'pin, G. B. *Chem. Rev.* **1997**, *97*, 2879. (f) Shilov, A. E. *Activation of Saturated Hydrocarbons by Transition Metal Complexes*; D. Riedel: Dordrecht, The Netherlands, 1984. (g) Shilov, A. E.; Shul'pin, G. B. *Activation and Catalytic Reactions of Saturated Hydrocarbons in the Presence of Metal Complexes*; Kluwer: Boston, 2000. (h) Arndtsen, B. A.; Bergman, R. G.; Mobley, T. A.; Peterson, T. H. *Acc. Chem. Res*. **1995**, *28*, 154.